# The di-iron RIC protein (YtfE) of *Escherichia coli* interacts with the DNA-binding protein from starved cells (Dps) to diminish RIC-protein-mediated redox stress

Liliana S.O. Silva[1], Joana M. Baptista[1], Charlotte Bately[2], Simon C. Andrews[2], and Lígia M Saraiva[1,*]

[1]Instituto de Tecnologia Química e Biológica NOVA, Av. da República, 2780-157 Oeiras, Portugal

[2] School of Biological Sciences, Knight Building, University of Reading, Reading RG6 6AJ, UK

*Corresponding author:

Lígia M. Saraiva

Av. da República, 2780-157 Oeiras, Portugal

Phone: +351-214469328; Fax: +351-214411277

E-mail: lst@itqb.unl.pt

## Abstract

The RIC (Repair of Iron Clusters) protein of *E. coli* is a di-iron hemerythrin-like protein that has a proposed function in repairing stress-damaged iron-sulphur clusters. To further understand the mechanism of action of RIC, we performed a Bacterial Two Hybrid screen of RIC-protein interaction partners in *E. coli*. As a result, the *E. coli* Dps was identified and its potential interaction was confirmed by further BACTH assays and by Bimolecular-Fluorescence-Complementation assay. The *ric* and *dps* single mutants displayed sensitivity to NO and $H_2O_2$ induced stress, respectively, whereas the *ric dps* double mutant displayed sensitivity to both stresses at similar levels to those seen for the corresponding single mutants. The activity of the Fe-S-containing aconitase enzyme was assayed as an indicator of cellular Fe-S cluster damage. Results showed significant loss of activity under non-stress conditions for the two single mutants, however, the double mutant displayed no loss of aconitase activity with respect to the wild type. Furthermore, complementation of the *ric dps* double mutant with multicopy *ric* led to a severe loss of aconitase activity, but this effect was not observed when a gene encoding a di-iron site variant of the RIC protein was employed. In addition, the *dps* mutant exhibited a large increase in ROS levels, but this increase was eliminated when *ric* was also inactivated. Absence of other iron-storage proteins, or of peroxidase and catalases had no impact of RIC-mediated redox stress induction. In summary, the results indicate that Dps and RIC proteins interact to counter RIC-protein-induced ROS.

## Importance

The mammalian immune system produces reactive oxygen and nitrogen species that kill bacterial pathogens by damaging key cellular components such as lipids, DNA and proteins. However, bacteria possess detoxifying and repair systems that mitigate such deleterious effects. The *E. coli* RIC (Repair of Iron Clusters) protein is a di-iron hemerythrin-like protein that repairs stress-damaged iron-sulphur clusters. *E. coli* Dps is an iron-storage protein of the ferritin superfamily with DNA-binding that protects cells from oxidative stress. We show that the RIC and Dps proteins interact in a fashion that counters RIC-protein-induced ROS. Altogether, the results unveil the formation of a new bacterial protein complex and reveal a novel contribution for Dps in bacterial redox-stress protection.


## Keywords

*E. coli*, di-iron RIC protein, YtfE, Dps, oxidative stress, nitrosative stress


## Running Title

Di-iron RIC protein interacts with Dps

## Introduction

During the infection process, bacterial pathogens are able to survive aggressive environments through the activation of specific stress-resistance genes. One such example of a stress-induced gene is *ric*. This gene encodes the 'Repair of Iron Centre' (RIC) protein that contains a di-iron centre and contributes to the protection of bacterial pathogens such as *Escherichia coli*, *Haemophilus influenzae*, *Salmonella* spp., *Yersinia* spp. and *Clostridium* spp. during exposure to nitrosative and/or oxidative stress (1). *ric* is induced upon exposure to either oxidative or nitrosative stress and in *E. coli, Staphylococcus aureus, Neisseria gonorrhoeae, H. influenza* and *Cryptococcus neoformans* the RIC protein is thought to confer stress resistance through maintenance of the activity of various Fe-S containing enzymes (1–3). Such an effect is well demonstrated for *E. coli* and *S. aureus* where RIC proteins restore the activity of oxidatively and nitrosatively-damaged Fe-S clusters in the TCA cycle enzymes, fumarase and aconitase (1, 4). In *E. coli*, the RIC protein also acts under non-stress conditions to maintain aconitase and fumarase activities (5). Further, the *E. coli* RIC protein delivers iron (most likely in the ferrous state) for the assembly of Fe-S clusters in spinach apo-ferredoxin and in the *E. coli* Fe-S cluster-assembly scaffold protein, IscU (6). The RIC protein also contributes to the survival of *S. aureus* and *H. influenzae* in activated macrophages, and is required for full virulence in *S. aureus* when infecting the wax moth larva infection-model, *Galleria mellonella* (3, 7). Thus, the RIC protein has an apparent role in bacterial pathogenicity through mediation of Fe-S cluster stability during exposure to redox- and/or nitrosative-stress.

The RIC proteins of *E. coli* and *S. aureus* contain di-iron centres of the histidine/carboxylate type within a four-helix-bundle fold (8). The UV-visible spectrum of

oxidized RIC protein exhibits a broad band at *ca.* 350 nm and Electron Paramagnetic Resonance (EPR) spectroscopy indicates that the principal g-values are below 2 (g=1.96, 1.92 and 1.88), which is indicative of a S=½ spin state in a mixed valence and anti-ferromagnetically coupled Fe(III)-Fe(II) binuclear iron centre. Mössbauer spectroscopy showed that the mixed-valence Fe(III)–Fe(II) di-iron centre of the RIC protein is more labile than that of the μ(oxo)-diferric form (6).

RIC proteins possess several highly-conserved amino acid residues of which some have been shown to influence the properties of the di-iron centre and/or function of the protein. In particular, substitution of residues His129, Glu133 or Glu208 of the *E. coli* RIC protein abrogated its ability to protect the Fe-S cluster of aconitase. Moreover, two μ-carboxylate bridges contributed by Glu133 and Glu208, linking the two di-iron site atoms, were shown to be required for the assembly of a stable di-iron centre (9). These studies also demonstrated the important contribution of the conserved His84, His129, His160, His204, Glu133 and Glu208 residues in ligating the di-iron centre within the four-helix bundle fold, and these di-iron coordination roles were recently confirmed by X-ray crystallographic structural studies (10).

In the work reported here, we sought to identify proteins that interact with, and support the function of, the RIC protein of *E. coli*. For this purpose, an *E. coli* library was screened for RIC protein interaction partners using the Bacterial Adenylate Cyclase Two Hybrid system (BACTH). Potential interacting gene products were further tested by BACTH and Bimolecular Fluorescence Complementation (BiFC) assays. Our protein-protein interaction studies revealed that the RIC protein interacts with the DNA-binding protein from starved

cells (Dps). Dps is a symmetrical dodecameric iron-storage protein of the ferritin superfamily that contains a di-iron ferroxidation centre located at the interface between subunits (11–13). Dps sequesters ferrous iron, which is oxidized preferentially by hydrogen peroxide at its di-iron centre and then deposited for storage as Fe(III) oxyhydroxide in the central cavity as an iron core; the sequestered iron can subsequently be released by reduction (13, 14). The ferroxidase activity, DNA-binding and iron-sequestration properties of Dps confer cells with protection from oxidative stress and nutrient deprivation, as judged by the reduced survival of *dps* mutants under stress conditions including starvation, oxidative stress, metal toxicity, and thermal stress (15). The physiological relevance of the interaction between the RIC protein and Dps was examined and the results revealed that Dps modulates the function of RIC.

## Results

### Identification of novel potential RIC-protein-interaction partners by screening a bacterial two-hybrid *E. coli* library

We used a genetic approach to further assess the physiological role of RIC in *E. coli,* in which a bacterial two-hybrid (BACTH) system (16) was employed to screen the *E. coli* genome for gene products that could interact with RIC. For this purpose, RIC was fused to C-terminal of *B. pertussis* adenylate cyclase T25 fragment and used as 'bait' to screen previously constructed partial-*Sau*3A-digested *E. coli* DNA random libraries that express fusions to the N-terminal of *B. pertussis* adenylate cyclase T18 fragment (17). We isolated 22 positive recombinant $Lac^+$ colonies, from which plasmids were purified and then transformed into *E. coli* DHM1 harbouring either pKT25-RIC or the empty vector pKT25 (control), and the β-galactosidase specific activities were determined (Figure 1). Seven pKT25-RIC transformants, harbouring plasmids A to G, exhibited significant β-galactosidase activity indicative of a specific interaction (Figure 1). Nucleotide sequencing followed by BLAST analysis was used to identify the genes within the inserts of these plasmids. Sequencing data revealed that plasmids A to C contain an ~2 kb *E. coli* DNA fragment upstream of the T18 Cya domain, and all contained the complete *efp* and *ecnA* genes, and part of the *ecnB* gene. The *efp* gene encodes the elongation factor EF-P, a translation factor that facilitates the *in vitro* the formation of the first peptide bond during translation (18, 19). The gene cluster *ecnAB* expresses two small cell-membrane associated entericidin lipoproteins, forming EcnAB a toxin-antitoxin module that regulates a

programmed bacterial cell death under high osmolarity conditions, with EcnA acting as the antidote for the bacteriolytic entericidin, EcnB (20).

The other four plasmids D to G also contained a ~2 kb insert located upstream of the T18 Cya domain, but in these cases the inserts carried the entire *rhtA* gene), encoding an inner-membrane transporter involved in resistance to homoserine/threonine (21), and the *dps* gene, encoding the DNA-binding and iron-storage protein from *s*tarved cells (11). Like RIC, *E. coli* Dps has been implicated in oxidative-stress protection, which raises the possibility of a functional association between these two proteins which might be dependent on their direct interaction. For this reason, the potential interaction between the two proteins was investigated further in order to establish its validity and determine its physiological purpose.

**The *E. coli* RIC protein interacts with Dps**

To determine whether the interaction between the RIC protein and Dps, as identified through the screening of the pUT18 library, is indeed genuine, further BACTH experiments were performed. To enable such experiments, the gene encoding the RIC protein was cloned into pUT18C and pUT18 vectors (to create T18-RIC and RIC-T18 fusions), and the *dps*-coding region was introduced into the pKNT25 vector (to give Dps-T25 fusions), following which the β-galactosidase activities of the corresponding co-transformants were measured. High β-galactosidase activities were recorded for both sets of the RIC-Dps BATCH combinations tested, with activities 4-6 times greater than those of the controls (Figure 2), indicative of interaction between the RIC protein and Dps within the cytosol of *E. coli*.

A second approach was also used to test the proposed RIC-Dps interaction, which involved using the Bimolecular Fluorescence Complementation (BiFC) assay. In this method, one of the two proteins of interest is fused to the N-terminal half of the green fluorescent protein (GFP), and the other protein of interest is fused to the C-terminal half; the assay depends upon an interaction between the two proteins that promotes the reassembly of the two halves of GFP such that emission of fluorescence is restored (22). Thus, GFP fusions (both the N- and C-terminal domains) were generated for both the RIC protein and Dps, and the fluorescence intensity of the corresponding *E. coli* cells containing plasmids co-expressing the RIC and Dps fusions was measured (Figure 3). The data show that cells expressing $RIC^{C\text{-}GFP}$ and $Dps^{N\text{-}GFP}$ exhibited an approximately six-fold higher fluorescence relative to the control, although transformants expressing $RIC^{N\text{-}GFP}$ and $Dps^{C\text{-}GFP}$ presented fluorescence levels similar to that of the control samples.

The RIC protein consists of two domains: a short N-terminal 'ScdA_N' domain of ~60 residues of unclear function with a highly-conserved pair of Cys residues (10); and a larger C-terminal 'hemerythrin' domain of ~140 residues that forms a di-iron centre. Therefore, we tested the BiFC interaction between Dps and a truncated form of RIC that lacks the so-called first Scd_N domain to determine which of the two RIC protein domains is responsible for the observed interaction with Dps. The results showed that the degree of interaction between the truncated RIC protein and Dps is similar to that observed when using the full-length protein (Figure 3). Thus, the interaction observed here between the RIC protein and Dps appears to be mediated through the C-terminal hemerythrin domain of the RIC protein.

**Dps modulates the function of the RIC protein in maintaining Fe-S cluster status**

The RIC protein has been linked to the resistance of *E. coli* to nitrosative and oxidative stresses as its inactivation decreases the survival of *E. coli* upon exposure to hydrogen peroxide or nitric oxide donors (4). Due to the interaction of the RIC and Dps proteins shown above, we questioned whether Dps could contribute to the stress protection afforded by the RIC protein. To test this possibility, a Δ*dps* Δ*ric* double mutant was constructed and the growth of *E. coli* wild type, Δ*ric*, Δ*dps*, Δ*dps* Δ*ric* mutants under oxidative and nitrosative stress conditions was tested (Figure 4). The growth experiments showed that inactivation of *ric* resulted in impaired growth under stress conditions imposed by 4 mM $H_2O_2$ or 250 µM spermine NONOate (Figure 4), which is consistent with previous reports (4). However, the *dps* mutation had little impact on growth under these conditions. Combining the Δ*dps* mutation with the Δ*ric* mutation did not result in any further growth reduction under the same stress conditions, i.e. the Δ*dps* Δ*ric* strain grew similarly to the Δ*ric* strain under the oxidative and nitrosative stress conditions employed (Figure 4). Thus, Dps does not notably compensate for the lack of the RIC protein under peroxide or NO-induced stress.

Another characteristic of the *E. coli ric* mutant is a reduced endogenous activity of Fe-S cluster-containing proteins, such as aconitase, that possess exposed Fe-S clusters exhibiting a marked sensitivity to redox and nitrosative stress (4). Therefore, the possible contribution of Dps to this phenotype was explored by comparing the aconitase activity of the Δ*dps* and Δ*dps* Δ*ric* strains to that of the wild type and Δ*ric* mutant. The results showed that the Δ*dps* mutation caused a 50% reduction in aconitase activity in log phase (Figure 5A), consistent with a role for Dps in maintaining Fe-S cluster status. As expected, a similar effect was

seen for the Δ*ric* mutant, although the activity reduction (30%) was only approximately half as great as that observed for the Δ*dps* mutant (Figure 5A). Surprisingly, the Δ*dps* Δ*ric* mutant exhibited aconitase activity that was higher than that of the corresponding single mutants and similar to that of the wild type (Figure 5A). These observed aconitase-activity effects were apparent in both the early-log and the post-exponential phase ($OD_{600}$ 0.6 and 2, respectively; Figure 5A and B), suggesting that the phenotype is independent of growth stage (note that *dps* is stationary-phase induced). The observed restoration of aconitase activity resulting from the combination of the *dps* and *ric* mutations suggests that the negative impact of lack of the RIC protein on such activity is dependent on the presence of Dps (and vice-versa), and this in turn indicates a hitherto unrecognised functional interdependence for these two proteins.

The association of the above aconitase-activity effects with the RIC protein was confirmed by complementation using a multicopy plasmid bearing the wild type *ric* gene under control of its natural promoter. Complementation of the single Δ*ric* mutant led to the recovery of aconitase activity to levels similar to those of the wild type (Figure 5C). More importantly, provision of a wild type version of *ric* (in multicopy) caused a large (60%) and significant reduction in the aconitase activity of the Δ*dps* Δ*ric* double mutant (Figure 5C). Thus, as anticipated, the *ric*-complemented double mutant exhibited the same phenotype as the *dps* mutant. This confirms that the RIC protein is responsible for decreasing aconitase activity in a $dps^-$ background.

To confirm that the role of the RIC protein in lowering aconitase activity in the *dps* mutant is dependent on a biochemically-functional version of the RIC protein, the ability of a RIC protein variant (lacking a complete di-iron site due to an E133L substitution; (9)), was used

in the complementation experiments (Figure 5C). The resulting activity data clearly show that the non-functional Glu133Leu-RIC variant does not lead to a notable decrease in aconitase activity when expressed in the Δ*dps* Δ*ric* strain (Figure 5C).

In summary, the above data suggest that in the absence of Dps, the RIC protein has a deleterious effect on aconitase activity, but that such an effect is not exhibited when Dps is present. This would imply that the interaction between Dps and the RIC protein, as revealed here, acts to ensure that neither of these two proteins can participate in processes that negatively impact the activity of aconitase.

**RIC does not interact with other *E. coli* iron-storage proteins**

*E. coli* Dps is an iron-sequestering protein composed of 12 identical subunits forming a shell surrounding a central cavity where up to ~500 ferric iron atoms can be sequestered. As *E. coli* encodes two other iron-storage proteins, namely bacterioferritin (Bfr) and ferritin (FtnA), the possibility that the RIC protein might also interact with these other iron-storage proteins was also investigated. Thus, corresponding BiFC experiments were performed in cells carrying recombinant plasmids that express the RIC protein with either Bfr or FtnA, as N- or C-terminal fusions to GFP domains. The resulting fluorescence intensity data failed to support any protein-protein interaction between the RIC protein and Bfr or FtnA (Figure 6A).

In a second set of experiments, the aconitase activity of wild type, Δ*ric*, Δ*bfr*, Δ*ftnA*, Δ*bfr* Δ*ric* and Δ*ftnA* Δ*ric* strains, grown to the exponential phase ($OD_{600}$ of 0.6), was determined. Similarly to the Δ*dps* strain, the Δ*bfr* and Δ*ftnA* strains both displayed ~50% lower aconitase activity levels (Figure 6B). But contrary to the effect of combining the Δ*dps* and Δ*ric* mutations, the combined absence of the RIC protein and the Bfr or FtnA proteins resulted in aconitase activities similar to those present in the correspondent single mutant strains (Figure 6B). Thus, the lower aconitase activity caused by the Δ*ric* mutation is not additive with respect to lower activity of resulting from the Δ*bfr* or Δ*ftnA* mutations. Further, it can be concluded that (unlike Dps) Bfr and FtnA do not tightly interact with the RIC protein, and that their absence does not result in a RIC-protein dependent decrease in aconitase activity.

**The RIC protein increases intracellular ROS levels when Dps is absent**

Dps protects cells from oxidative stress due to its ability to couple the reduction of hydrogen peroxide to water with the oxidation of free-ferrous iron to sequestered-ferric iron. In addition, its association with DNA helps to prevent ROS-induced DNA damage (23). This suggests that the role of Dps in preventing RIC-protein induced inhibition of aconitase activity may arise from the ability of Dps to detoxify ROS that might be produced by the di-iron centre of the RIC protein (e.g. through binding and reduction of oxygen). Therefore, the ROS content of Δ*ric*, Δ*dps* and Δ*dps* Δ*ric* strains were compared with those found in the wild type to determine whether the presence of the RIC protein, in the absence of Dps, results in raised levels of ROS (Figure 7). The results show that the wild type and

286 Δ*ric* mutant contain similar amounts of ROS while the Δ*dps* strain had significantly higher
287 (~2-fold) levels (Figure 7). This is as expected given the known role of Dps in redox-stress
288 resistance (23). However, introduction of the *ric* mutation into the *dps* mutant eliminated
289 the increased intracellular ROS levels of the single Δ*dps* mutant (Figure 7). This suggests
290 that the raised ROS levels of the *dps* single mutant are a consequence of an increase in
291 RIC-protein-dependent ROS production which thus supports a role for Dps in interacting
292 with the RIC protein to restrict its release of ROS species.

293 To discover whether other elements of the redox-stress resistance response might also act to
294 lessen RIC-protein induced ROS production, the Δ*ric* mutation was introduced into a strain
295 (Δ*hpx*) lacking capacity to degrade hydrogen peroxide due to inactivation of both catalase
296 genes as well as the alkyl-hydroperoxide reductase genes (Table 1; (24, 25) . Assay of the
297 resulting aconitase activity levels showed that the Δ*hpx* Δ*ric* quadruple mutant has activity
298 levels similar to those determined for the Δ*ric* and Δ*hpx* mutants (Figure 8), which shows
299 that the three major peroxidases (KatE, KatG, AhpCF) of *E. coli* are not involved in
300 countering any RIC-protein mediated ROS production, at least under conditions where Dps
301 is active.

302

303

304

305

306

## Discussion

Aconitase and fumarase are enzymes of the TCA cycle that are prone to oxidative stress damage. We previously showed that the di-iron RIC protein repairs these enzymes and is able to transfer iron to Fe-S containing proteins (4–6). In the work described here, we screened an *E. coli* BACTH library in order to identify proteins that interact with the RIC protein and thus might be required to assist its function. As a consequence of our screening, Dps emerged as a RIC protein interaction candidate. This suggested interaction was supported by generation and analysis of additional Dps and RIC protein BACTH constructs and by a GFP complementation assay. Dps belongs to the ferritin superfamily which led us to investigate the possible interaction of RIC with the two other ferritins present in *E. coli*, namely ferritin and bacterioferritin. However, neither of these proteins were found to interact with the RIC protein or to influence its activity *in vivo*.

We also observed that inactivation of the RIC protein resulted in lower aconitase activity, which is consistent with previous findings indicating that this protein contributes to the protection of solvent accessible Fe-S clusters from ROS damage under aerobic growth conditions (5). Similar results were herein obtained for the single mutant strains of *dps*, *ftnA* and *bfr*, indicating that lack of any of these gene products results in lower endogenous aconitase activity. The role of FtnA and Bfr in aconitase protection was previously demonstrated as the two ferritins promote the reactivation of aconitase activity following stress damage in *Salmonella enterica* serovar Typhimurium (26). In contrast with our findings with *E. coli*, no loss of aconitase activity was observed for *S. enterica ftnA* or *bfr* single mutants in the absence of stress; this discrepancy may be related to the different function and regulation of ferritins in *Salmonella* and *E. coli* species (26, 27).

A surprising result was the finding that the defective aconitase activity of the Δ*dps* and Δ*ric* single-mutant strains was reversed when these two mutations were combined in the Δ*dps* Δ*ric* double mutant, such that activity was restored to that seen in the wild type. This result, together with the lower amounts of ROS observed in the Δ*dps* Δ*ric* mutant compared to the Δ*dps* mutant, suggests that the RIC protein is responsible for the generation of ROS, but only in the absence of Dps and, thus, that the interaction of Dps and the RIC protein serves to enable Dps to restrict ROS release (which is presumed to damage the Fe-S cluster of aconitase and hence lower the observed activity of this enzyme in a *dps* mutant) by the RIC protein. Interestingly, other redox-stress resistance components (KatE, KatG and AhpCF) failed to impact the RIC-protein-mediated inhibition of aconitase activity (at least in the presence of Dps). These results suggest that the effect of Dps on the ROS-generation activity of the RIC protein is one that is highly specific and not replicated by the other peroxide-consuming cytosolic factors examined. Indeed, the findings relayed here indicate that a direct interaction is required to enable Dps to quench the ROS-generating activity of the RIC protein. The exact mechanism involved in the apparent quenching of RIC-protein-mediated ROS production by Dps is unclear; such understanding will require in vitro reaction studies combining the Dps and RIC proteins. However, two possible processes by which Dps could exert a ROS-quenching action upon the RIC protein can be considered: Dps might sequester iron released from the di-iron site of the RIC protein and thus restrict Fe-driven Fenton chemistry; or Dps could consume hydrogen peroxide (or hydroxyl radicals; (14, 28)) generated by the RIC protein through reaction at its di-iron site with molecular oxygen.

The absence of the RIC protein also reduced aconitase activity, but only in the presence of Dps. However, lack of RIC protein had no impact on ROS levels when Dps was present. The reason for this effect is unclear but may indicate a role for the RIC protein in supply of iron from Dps for Fe-S cluster repair and/or synthesis.

The proposed role of the RIC protein (4) is to repair damaged Fe-S clusters of [Fe-S]-proteins, such as aconitase and fumarase, by donating iron from its di-iron centre leading to the formation of an intermediate mononuclear iron centre that is prone to react with oxygen to generate ROS such as hydrogen peroxide. In this process, the interaction with Dps would fulfil two roles, namely by trapping ROS released by the RIC protein and providing a sink for iron liberated from the di-iron centre of RIC.

In conclusion, we report an interaction between the Dps and RIC proteins of *E. coli* which represents the first example of a protein that interacts with the ferritin-like Dps protein. In addition, our results indicate that the Dps-RIC protein interaction contributes to the function of RIC, which is one of the few known bacterial repairing proteins.

## Materials and Methods

### *Bacterial strains and growth conditions*

*Escherichia coli* strains used in this work are listed in Table 1, and all were grown at 37 °C. *E. coli* reporter strain DHM1 non-reverting adenylate cyclase deficient (*cya*) was used for detection of protein-protein interactions and *E. coli* XL2Blue was used as host strain.

Construction of the *E. coli* double mutant strains was performed by bacteriophage P1-mediated transduction (29), and the corrected mutations were confirmed by PCR using primers listed in Table 2.

*E. coli* cells were grown in LB medium under aerobic conditions in flasks containing a 1/5 volume of culture or under anaerobic conditions in rubber seal-capped flasks filled with medium and extensively bubbled with nitrogen prior to growth. For the stress assays, cells were grown, at 37 °C and 150 rpm, in M9B minimal medium (60 mM $K_2HPO_4$, 33 mM $KH_2PO_4$, 7.6 mM $(NH_4)_2SO_4$, 1.7 mM sodium citrate, 1 mM $MgSO_4$ and 10 µM $MnCl_2$, pH 7) supplemented with 10 µg/mL thiamine and 40 µg/mL L-arginine, L-leucine, L-proline, L-threonine and 40 mM glucose. Once cultures reached an $OD_{600}$=0.3, they were either left untreated or exposed to 4 mM $H_2O_2$ for 6 h or to 250 µM spermine-NONOate for 9 h.

### *BACTH experiments*

The Bacterial Adenylate Cyclase-based Two-Hybrid (BACTH) system assay (16) was used to identify RIC -interacting proteins. *E. coli*RIC protein was fused to the C-terminal of

392 *Bordetella pertussis* Cya (adenylate cyclase) T25 domain (pKT25-RIC) and used to screen
393 an *E. coli* MC4100 gene library containing chromosomal fragments fused to the N-terminal
394 of *B. pertussis* Cya T18 domain. The DNA fragments were obtained by partial digestion
395 with *Sau*3AI and cloning into the *Bam*HI site of pUT18 plasmids (17). About 1 µg of
396 pUT18*Bam*HI DNA library was transformed together with pKT25-RIC into *E. coli* DHM1
397 cells by electroporation. Blue colonies present in $Amp^R$ $Cm^R$ selective plates (L-agar with
398 5-bromo-4-chloro-3-indolyl β-D-galactopyranoside (X-Gal)) were identified after
399 incubation at 30 $^oC$ for 36 h, and cells with the highest β-galactosidade were considered to
400 contain recombinant plasmids harbouring genes encoding polypeptides that interact with
401 the *E. coli* RIC protein. Twenty two colonies were obtained and the corresponding plasmids
402 were isolated, co-transformed with pKT25-RIC plasmid in *E. coli* DHM1 and the strength
403 of the protein-protein interactions observed was again estimated by quantification of β-
404 galactosidase activity. Seven isolates considered positive were named 'A' to 'G' (Figure 1)
405 and subject to nucleotide sequencing using primer $T18_{Fw}$ (Table 2). The sequences
406 obtained were screened against the *E. coli* K-12MG1655 genome using BLAST to identify
407 the encoded genes.
408 Genes coding for the RIC protein and Dps were PCR amplified from *E. coli* K-12 genomic
409 DNA using the oligonucleotides described in Table 2, and cloned into pKT25 (fused to Cya
410 C-terminal T25 domain), pKNT25 (fused to Cya N-terminal T25 domain), pUT18 (fused to
411 Cya N-terminal T18 domain) and pUT18C (fused to Cya C-terminal T18 domain)
412 plasmids, and the enzyme *Pfu* DNA polymerase (Thermo Scientific). The resulting
413 recombinant plasmids encoded either Dps or the RIC protein with either a C- or N-
414 terminally linked T25 or T18 domain from the *B. pertussis* Cya) protein. Two
415 complementary plasmids, one carrying a T25 fragment and the other a T18 fragment, were

co-transformed into the *E. coli* DHM1 strain (*cya*$^-$). *E. coli* DHM1 cells containing the *ric*-encoding pUT18 or pUT18C plasmids were co-transformed with complementary pKTN25 empty plasmid to provide negative controls.

In all cases, false positives were tested by co-transformation of *E. coli* DHM1 with plasmids containing each gene and pKT25-TorD, which expresses *E. coli* TorD that binds non-specifically to a wide variety of polypeptides (30).

For β-galactosidase activity determination (31), at least 3 representative colonies of each transformation plate were inoculated, in duplicate, in LB medium, and following an overnight growth at 37 °C, transformant cultures were re-inoculated (at a 0.01 dilution) into LB with ampicillin (100 μg/mL), kanamycin (50 μg/mL) and IPTG (0.5 mM). When cultures reached an $OD_{600}$=0.5 (approximately after 16 h of growth, at 30 °C), 1 mL of each culture was collected by centrifugation (5 min, 5000 *g*, 4 °C). The pellets were lysed by incubation with 100 μL BugBuster HT 1x (Novagen) at 37 °C, for 30 min. Cellular debris was then removed by centrifugation and β-galactosidase activity was assayed in 20 μL suspensions in a microplate reader. The assays were initiated by addition of a reaction mixture comprising: 0.27% β-mercaptoethanol (v/v) and 0.9 mg/mL ONPG (o-nitrophenyl-β-D-galactopyranoside) in buffer A (60 mM $Na_2HPO_4.7H_2O$, 40 mM $NaH_2PO_4.H_2O$, 1 mM $MgSO_4.7H_2O$, 10 mM KCl). Reactions were incubated at 28 °C, and absorbance was recorded at 420 nm at 2 min intervals, for 90 min. The β-galactosidase specific activity was defined in ONP/min/milligram of protein. Interactions were considered positive for those reactions where β-galactosidase activity was at least four times higher than the negative control.

*Bimolecular fluorescence complementation (BiFC) assays*

BIFC assay was performed essentially as described previously (32). For this purpose, the genes encoding RIC protein, a truncated version of the RIC protein (lacking the first 57 amino acid residues in N-terminal (9)) Dps, Bfr and FtnA were PCR amplified from genomic DNA of *E. coli* K-12 using the primers described in Table S2, and the DNA fragments were cloned into vectors (pET11a-link-N-GFP and pMRBAD-link-C-GFP; (32) that express the green fluorescence protein, GFP, to allow formation of corresponding N- or C-terminal GFP fusions. Cloning was achieved using *Xho*I and *Bam*HI sites (for cloning into pET11a-link-N-GFP) or *Nco*I and *Aat*II (for cloning into pMRBAD-link-C-GFP) sites, except for Dps for which *Sph*I replaced *Nco*I. All recombinant plasmids were sequenced confirming the integrity of the genes and the absence of undesired mismatches. Cells harboring pET11a-link-N-GFP and pMRBAD-link-C-GFP served as negative control.

*E. coli* BL21(DE3)Gold (Stratagene) was co-transformed with the resulting recombinant pET11a-link-N-GFP and pMRBAD-link-C-GFP vectors, in various combinations (RIC/Dps, truncated-RIC/Dps, RIC/Bfr and RIC/FtnA), and plated on selective LB-agar. Colonies were inoculated in LB medium, grown overnight, at 37 $^{o}$C and 150 rpm, and plated in inducing medium containing 20 µM IPTG and 0.2 % of arabinose. After an overnight incubation at 30 $^{o}$C followed by two days incubation at room temperature, colonies were suspended in PBS and spread on 1.7% agarose slides. Cells were examined for green fluorescence in a Leica DM6000 B upright microscope coupled to an Andor iXon+ camera, using 1000x amplification and a FITC filter. The images were analysed using the MetaMorph Microscopy Automation and Image Analysis Software.

*Aconitase activity assays and determination of endogenous ROS*

All *E. coli* strains were grown, from an overnight inoculum, in LB medium under aerobic conditions and 37 °C, until reaching an $OD_{600}$ of either 0.6 or 2, as indicated. Cells were collected, washed in reaction buffer (50 mM Tris-HCl, 0.6 mM $MnCl_2$, pH 8) and frozen in liquid nitrogen. Cell extracts were prepared under anaerobic conditions, by suspending the cell pellets in reaction buffer containing 0.5 mg/mL lysozyme and 0.2 mg/mL DNAse, and then incubating on ice for 10 min. Supernatants were obtained by centrifugation at 9600 *g* for 10 min at 4 °C, and aconitase activity was then determined in by reaction with 200 µM $NADP^+$, 1 U isocitrate dehydrogenase and 30 mM sodium citrate (9) by following the formation of NADPH at 340 nm. Wild type and Δ*ric*, Δ*dps* and Δ*dps* Δ*ric* strains of *E. coli* were transformed with either pUC18, pUC18-RIC or pUC18-RIC-E133L (described in (9)) and were similarly tested for endogenous aconitase activity.

Endogenous reactive oxygen species content was determined in wild type, Δ*ric*, Δ*dps*, Δ*dps* Δ*ric*, Δ*bfr*, Δ*bfr* Δ*ric*, Δ*ftnA*, Δ*ftnA* Δ*ric* strains *E. coli* (Table 1). Cells were grown aerobically to an $OD_{600}$=0.6, collected by centrifugation, resuspended in PBS, and distributed in 96-well microtitre plates. Following the addition of dichloro-dihydro-fluorescein diacetate (10 µM DCFH-DA,), fluorescence was evaluated ($\lambda_{ex}$ = 485 nm and $\lambda_{em}$ = 538 nm) for 2 h in a spectrofluorimeter Varian Cary (Agilent). The Fluorescence Intensity (FI) was normalized in relation to the optical density of each culture at 600 nm.

## Acknowledgments

We thank Professor Hirotada Mori (Graduate School of Biological Sciences, Nara Institute of Science and Technology, Ikoma, Nara, Japan) for provision of the Keio mutant collection, and Professor James Imlay (Department of Microbiology, B103 CLSL, 601 S Goodwin Ave, Urbana, IL 61801, USA) for the Hpx mutant.

The work was funded by Fundação para a Ciência e a Tecnologia (FCT) project PTDC/BBBBQB/5069/2014 and by the FCT fellowship SFRH/BD/118545/2016 (L. Silva). The funders had no role in study design, data collection and interpretation, or the decision to submit the work for publication.

## References

1. Overton TW, Justino MC, Li Y, Baptista JM, Melo AMP, Cole JAa, Saraiva LM. 2008. Widespread distribution in pathogenic bacteria of di-iron proteins that repair oxidative and nitrosative damage to iron-sulfur centers. J Bacteriol 190:2004–13.

2. Chow ED, Liu OW, O'Brien S, Madhani HD. 2007. Exploration of whole-genome responses of the human AIDS-associated yeast pathogen *Cryptococcus neoformans* var grubii: nitric oxide stress and body temperature. Curr Genet 52:137–148.

3. Harrington JC, Wong SMS, Rosadini C V, Garifulin O, Boyartchuk V, Akerley BJ.

2009. Resistance of *Haemophilus influenzae* to reactive nitrogen donors and gamma interferon-stimulated macrophages requires the formate-dependent nitrite reductase regulator-activated *ytfE* gene. Infect Immun 77:1945–1958.

4. Justino MC, Almeida CC, Teixeira M, Saraiva LM. 2007. *Escherichia coli* di-iron YtfE protein is necessary for the repair of stress-damaged iron-sulfur clusters. J Biol Chem 282:10352–9.

5. Justino MC, Almeida CC, Gonçalves VL, Teixeira M, Saraiva LM. 2006. *Escherichia coli* YtfE is a di-iron protein with an important function in assembly of iron-sulphur clusters. FEMS Microbiol Lett 257:278–84.

6. Nobre LS, Garcia-Serres R, Todorovic S, Hildebrandt P, Teixeira M, Latour J-M, Saraiva LM. 2014. *Escherichia coli* RIC is able to donate iron to iron-sulfur clusters. PLoS One 9:e95222.

7. Silva LO, Nobre LS, Mil-Homens D, Fialho A, Saraiva LM. 2018. Repair of Iron Centers RIC protein contributes to the virulence of *Staphylococcus aureus*. Virulence 9:312–317.

8. Todorovic S, Justino MC, Wellenreuther G, Hildebrandt P, Murgida DH, Meyer-Klaucke W, Saraiva LM. 2008. Iron-sulfur repair YtfE protein from *Escherichia coli*: Structural characterization of the di-iron center. J Biol Inorg Chem 13:765–770.

9. Nobre LS, Lousa D, Pacheco I, Soares CM, Teixeira M, Saraiva LM. 2015. Insights into the structure of the diiron site of RIC from *Escherichia coli*. FEBS Lett 589:426–431.

10. Lo F-C, Hsieh C-C, Maestre-Reyna M, Chen C-Y, Ko T-P, Horng Y-C, Lai Y-C,

527 Chiang Y-W, Chou C-M, Chiang C-H, Huang W-N, Lin Y-H, Bohle DS, Liaw W-F.
528 2016. Crystal structure analysis of the Repair of Iron Centers Protein YtfE and its
529 interaction with NO. Chem - A Eur J 1–10.

530 11. Almiron M, Link J, Furlong D, Kolter R. 1992. A novel DNA-binding protein with
531 regulatory and protective roles in starved *Escherichia coli*. Genes Dev 6:2646–2654.

532 12. Grant R , Filman DJ, Finkel SE, Kolter R, Hogle JM. 1998. The crystal structure of
533 Dps, a ferritin homolog that binds and protects DNA. Nat Struct Biol 5:294–303.

534 13. Calhoun LN, Kwon YM. 2011. Structure, function and regulation of the DNA-
535 binding protein Dps and its role in acid and oxidative stress resistance in *Escherichia*
536 *coli*: a review. J Appl Microbiol 110:375–86.

537 14. Zhao G, Ceci P, Ilari A, Giangiacomo L, Laue TM, Chiancone E, Chasteen ND.
538 2002. Iron and hydrogen peroxide detoxification properties of DNA-binding protein
539 from starved cells. A ferritin-like DNA-binding protein of *Escherichia coli*. J Biol
540 Chem 277:27689–96.

541 15. Karas VO, Westerlaken I, Meyer AS. 2015. The DNA-Binding Protein from Starved
542 Cells (Dps) utilizes dual functions to defend cells against multiple stresses. J
543 Bacteriol 197:3206–15.

544 16. Karimova G, Pidoux J, Ullmann A, Ladant D. 1998. A bacterial two-hybrid system
545 based on a reconstituted signal transduction pathway. Proc Natl Acad Sci U S A
546 95:5752–5756.

547 17. Jack RL, Buchanan G, Dubini A, Hatzixanthis K, Palmer T, Sargent F. 2004.
548 Coordinating assembly and export of complex bacterial proteins. EMBO J 23:3962–

549 72.

550 18. Blaha G, Stanley RE, Steitz TA. 2009. Formation of the first peptide bond: The
551 structure of EF-P bound to the 70S ribosome. Science 80 325:966–970.

552 19. Ganoza MC, Aoki H. 2000. Peptide bond synthesis: function of the *efp* gene product.
553 Biol Chem 381:553–559.

554 20. Bishop RE, Leskiw BK, Hodges RS, Kay CM, Weiner JH. 1998. The entericidin
555 locus of *Escherichia coli* and its implications for programmed bacterial cell death. J
556 Mol Biol 280:583–596.

557 21. Livshits VA, Zakataeva NP, Aleshin V V., Vitushkina M V. 2003. Identification and
558 characterization of the new gene *rhtA* involved in threonine and homoserine efflux in
559 *Escherichia coli*. Res Microbiol 154:123–135.

560 22. Magliery TJ, Wilson CGM, Pan W, Mishler D, Ghosh I, Hamilton AD, Regan L.
561 2005. Detecting protein-protein interactions with a green fluorescent protein
562 fragment reassembly trap: Scope and mechanism. J Am Chem Soc 127:146–157.

563 23. Chiancone E, Ceci P. 2010. The multifaceted capacity of Dps proteins to combat
564 bacterial stress conditions: Detoxification of iron and hydrogen peroxide and DNA
565 binding. Biochim Biophys Acta 1800:798–805.

566 24. Park S, You X, Imlay JA. 2005. Substantial DNA damage from submicromolar
567 intracellular hydrogen peroxide detected in Hpx- mutants of *Escherichia coli*. Proc
568 Natl Acad Sci U S A 102:9317–9322.

569 25. Seaver LC, Imlay JA. 2004. Are respiratory enzymes the primary sources of
570 intracellular hydrogen peroxide? J Biol Chem 279:48742–50.

571 26. Velayudhan J, Castor M, Richardson A, Main-Hester KL, Fang FC. 2007. The role
572 of ferritins in the physiology of *Salmonella enterica* sv. Typhimurium: A unique role
573 for ferritin B in iron-sulphur cluster repair and virulence. Mol Microbiol 63:1495–
574 1507.

575 27. Abdul-Tehrani H, Hudson AJ, Chang YS, Timms AR, Hawkins C, Williams JM,
576 Harrison PM, Guest JR, Andrews SC. 1999. Ferritin mutants of *Escherichia coli* are
577 iron deficient and growth impaired, and fur mutants are iron deficient. J Bacteriol
578 181:1415–1428.

579 28. Bellapadrona G, Ardini M, Ceci P, Stefanini S, Chiancone E. 2010. Dps proteins
580 prevent Fenton-mediated oxidative damage by trapping hydroxyl radicals within the
581 protein shell. Free Radic Biol Med 48:292–297.

582 29. Lennox ES. 1955. Transduction of linked genetic characters of the host by
583 bacteriophage P1. Virology 1:190–206.

584 30. Pommier J, Mejean V, Giordano G, Iobbi-Nivol C. 1998. TorD, a cytoplasmic
585 chaperone that interats with the unfolded trimethylamine N-oxide reductase enzyme
586 (TorA) in *Escherichia coli*. J Biol Chem 273:16615–16620.

587 31. Thibodeau SA, Fang R, Joung JK. 2004. High-throughput β-galactosidase assay for
588 bacterial cell-based reporter systems. Biotechniques 36:410–415.

589 32. Wilson CGM, Magliery TJ, Regan L. 2004. Detecting protein-protein interactions
590 with GFP-fragment reassembly. Nat Methods 1:255–262.

591 33. Justino MC, Vicente JB, Teixeira M, Saraiva LM. 2005. New genes implicated in
592 the protection of anaerobically grown *Escherichia coli* against nitric oxide. J Biol

593 Chem 280:2636–43.

594 34. Baba T, Ara T, Hasegawa M, Takai Y, Okumura Y, Baba M, Datsenko KA, Tomita
595 M, Wanner BL, Mori H. 2006. Construction of *Escherichia coli* K-12 in-frame,
596 single-gene knockout mutants: the Keio collection. Mol Syst Biol 2.

597 35. Seaver LC, Imlay JA. 2001. Alkyl hydroperoxide reductase is the primary scavenger
598 of endogenous hydrogen peroxide in *Escherichia coli*. J Bacteriol 183:7173–81.

599 36. Jang S, Imlay JA. 2010. Hydrogen peroxide inactivates the *Escherichia coli* Isc iron-
600 sulphur assembly system, and OxyR induces the Suf system to compensate. Mol
601 Microbiol 78:1448–1467.

602

603

604 **Table 1 –Strains and plasmids used in this study**

605

| *E.coli* | Description | Source |
|---|---|---|
| **Strains** | | |
| DHM1 | F′, *cya-854, recA1, endA1, gyrA96* ($Nal^R$), *thi1, hsdR17, spoT1, rfbD1, glnV44(AS)* | Euromedex |
| Wild type | K-12 ATCC 23716 | ATCC |
| Δ*ric* | K-12 Δ*ric*::*cat* | (33) |
| Δ*dps* | JS091 Δ*dps*::*kan* | (34) |
| Δ*bfr* | JW3298 Δ*bfr*::*kan* | (34) |
| Δ*ftnA* | MC4100 Δ*ftnA*::*spc* | (27) |
| Δ*dps*Δ*ric* | K-12 Δ*dps*::*kan*, Δ*ric*::*cat* | This study |
| Δ*bfr*Δ*ric* | K-12 Δ*bfr*::*kan*, Δ*ric*::*cat* | This study |
| Δ*ftnA*Δ*ric* | K-12 Δ*ftnA*::*spc*, Δ*ric*::*cat* | This study |
| MG1655 | $F^-$ WT | (35) |
| SJ90 | BW25113 Δ*ric*::*cat* | (36) |
| LC106 (*hpx*) | Δ*ahpCF'kan*::*'ahpḞ*, Δ(*katG17*::Tn*10*)1, Δ(*katE12*::Tn*10*)1 | (25) |
| Δ*hpx*Δ*ric* | LC106 Δ*ric1*::cat | This study |
| XL2 Blue | *recA1, endA1, gyrA96, thi-1, hsdR17, supE44, relA1, lac* [F' *proAB*$^+$, *lacIqZ*ΔM15 Tn*10* ($Tet^r$)] | Stratagene |
| BL21Gold(DE3) | *E. coli* B, $F^-$, *ompT, hsdS* ($r_B^-$ $m_B^-$), *dcm*$^+$, $Tet^r$, | Stratagene |

| | | |
|---|---|---|
| | *gal*, *λ*(DE3), *endA*, Hte | |
| **Plasmids** | | |
| pUT18/pUT18C | Vector that allows construction of in-frame fusions at the N-terminus/C-terminus of T18 fragment (amino acids 225-399 of CyaA) | (16) |
| pKT25/pKNT25 | Vector that allows construction of in-frame fusions at the N-terminus/C-terminus of T25 fragment (amino acids 1-224 of CyaA) | (16) |
| pUT18/pUT18C-ric | RIC fused to T18 fragment in N/C-terminal | This study |
| pKT25/pKNT25-ric | RIC fused to T25 fragment in N/C-terminal | This study |
| pUT18/pUT18C-dps | Dps fused to T18 fragment in N/C-terminal | This study |
| pKT25/pKNT25-dps | Dps fused to T25 fragment in N/C-terminal | This study |
| pUT18-Zip | Leucine zipper fused to T18 fragment in the N-terminal | (16) |
| pKT25-Zip | Leucine zipper fused to T25 fragment in the C-terminal | (16) |
| pUT18-TorD | TorD fused to T18 fragment in N-terminal | (17) |
| pKT25-TorD | TorD fused to T25 fragment in C-terminal | (17) |
| BamHI | pUT18 plasmid that contains chromosomal fragments obtained by partial digest of the MC4100 chromosomal DNA with Sau3A1 and cloned into de BamHI site | (17) |

| | | |
|---|---|---|
| pUC18 | Expression vector | ATCC |
| pUC18-ric | Vector for expression of RIC | (4) |
| pUC18-RIC-Glu133Leu | Vector for expression of RIC-Glu133Leu | (9) |
| pET11a-link-GFP | Vector for expression of fusions with N-terminal fragment of GFP | (32) |
| pMRBAD-link-GFP | Vector for expression of fusions with C- terminal fragment of GFP | (32) |
| pET11a-ric-GFP | RIC fused to N-terminal GFP fragment | This study |
| pMRBAD-ric-GFP | RIC fused to C-terminal GFP fragment | This study |
| pET11a-dps-GFP | Dps fused to N-terminal GFP fragment | This study |
| pMRBAD-dps-GFP | Dps fused to C-terminal GFP fragment | This study |
| pET11a-bfr-GFP | Bfr fused to N-terminal GFP fragment | This study |
| pMRBAD-bfr-GFP | Bfr fused to C-terminal GFP fragment | This study |
| pET11a-ftnA-GFP | FtnA fused to N-terminal GFP fragment | This study |
| pMRBAD-ftnA-GFP | FtnA fused to C-terminal GFP fragment | This study |
| pET11a-ricTrunc-GFP | Truncated RIC fused to N-terminal GFP fragment | This study |
| pMRBAD-ricTrunc-GFP | Truncated RIC fused to C-terminal GFP fragment | This study |

606

607

608 **Table 2 – Oligonucleotides used in this study**

| Primer Name | Sequence |
|---|---|
| **Construction of plasmids used in BACTH** | |
| ric_Fw | GAGGTGTCGACTATGGCTTATC |
| ric_Rv | CTTTTAGGATCCTCACCCGCC |
| dps_Fw | GTTAATTACTGGGATCCAACATCAAGAGG |
| dps_Rv | TCCTGTCAGGTACCCGCTTTTATC |
| T18_Fw | CATTAGGCACCCCAGGCTTTAC |
| T18_Rv | GAGCGATTTTCCACAACAAGTC |
| T18C_Fw | CATACGGCGTGGCGGGGAAAAG |
| T18C_Rv | AGCGGGTGTTGGCGGGTGTCG |
| T25_Fw | ATGCCGCCGGTATTCCACTG |
| T25_Rv | CGGGCCTCTTCGCTATTACG |
| NT25_Fw | CACCCCAGGCTTTACACTTTATGC |
| NT25_Rv | CAATGTGGCGTTTTTTTCCTTCG |
| **Construction of plasmids used in BiFC** | |
| ric_xhoFw | GAATGAGGTCTCGAGTATGGCTTATC |
| ric_bamRv | GCGCAATGGGATCCAGCTTTTAGA |
| ric_ncoFw | GAGGTATCAGCCATGGCTTATCG |
| ric_aatRv | CCAGCTTTTAGACGTCTCACCC |
| dps_xhoFw | CGTTAATTACTCGAGCATAACATCAAG |
| dps_bamRv | GTACTAAGGATCCGCACCATCAGC |

| | |
|---|---|
| dps_sphFw | CAAGAGGATATGCATGCATGAGTACCGCTA |
| dps_aatRv | CATCAGCGATGGGACGTCTCGATGTTAG |
| bfr_xhoFw | GAGTGGAAGCGCTCGAGTCAAAAAATG |
| bfr_bamRv | GGAGGGTTCTGGATCCCGACACG |
| bfr_ncoFw | GAAGGAGTCAAACCATGGAAGGTGATAC |
| bfr_aatRv | CGGACGTCCCTTCTTCGCGGATC |
| truncric_xhoFw | CTTTAAGAAGGCTCGAGACATATGGCTG |
| truncric_ncoFw | GGAGATATACCCATGGCTGAACAAC |
| ftna_xhoFw | CAAATATAACCTTTCTCGAGCACTATC |
| ftna_bamRv | TGAAACGGATCCAGTAAACCTGC |
| ftna_ncoFw | GAGCACTACCATGGTGAAACCAGAAAT |
| ftna_aatRv | CGGAGAGGACGTCTTTTGTGTGTC |
| **Double mutant construction confirmation** | |
| Conf_dps_Fw | CAGAATAGCGGAACACATAGC |
| Conf_dps_Rv | GATGCACTAAATAAGTGCGTTG |
| Conf_bfr_Fw | CTCTTCAAAGAGTGGAAGCG |
| Cof_bfr_Rv | GATCTCTTATTAACCGGGAGG |
| Conf_ftnA_Fw | CAAATTATAGTGACGCCACAG |
| Conf_ftnA_Rv | ACCGATCAGAGTAAGATTTGC |
| Conf_ric_Fw | AAGAATGAGGTATCACATATGGCTTATCGC |
| Conf_ric_Rv | GGCTGTTTATTGGTAAGAATTCGGCTGCTG |

609

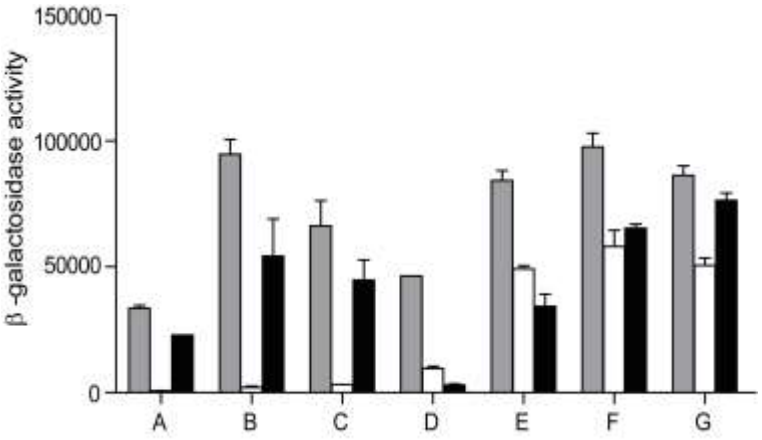


**Figure 1: *E. coli* RIC interactions analysed by BACTH.** β-Galactosidase activities of *E. coli* DHM1 cell lysates expressing, separately, plasmids A to G, which were extracted from two different *BamH*I libraries, and co-transformed with the pKTN25-RIC (grey bars), pKTN25 empty plasmid (white bars), and pKTN25 fused to TorD (black bars). Each bar represents the mean value ± standard error from results of at least three independent cultures.

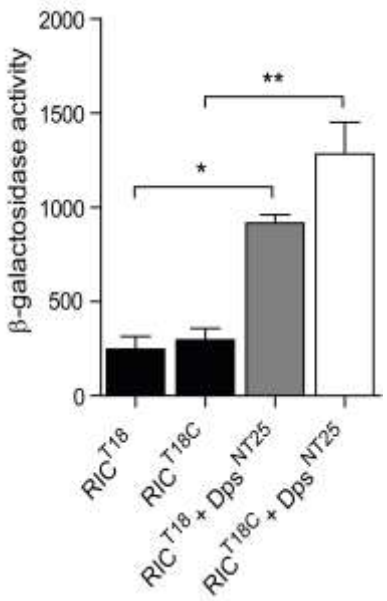


**Figure 2: Assessment of the interaction of the *E. coli* RIC and Dps proteins using the bacterial two-hybrid assay.** The interaction of the RIC protein, fused to the C- (white bar) or N-terminus (grey bar) of the T18-Cya domain and expressed from pUT18 or pUT18C, respectively, was evaluated in *E. coli* DHM1 co-transformed with pKTN25 containing a Dps fused to the N-terminus of the T25-Cya domain. *E. coli* cells harbouring simultaneously empty pKTN25 and pUT18/pUT18C vectors expressing *ric* fusions served as negative controls (black bars). Values are means (± standard error) of at least three independent cultures analysed in duplicate. *$p<0.05$; **$p<0.005$ (One-way ANOVA multiple comparison test).

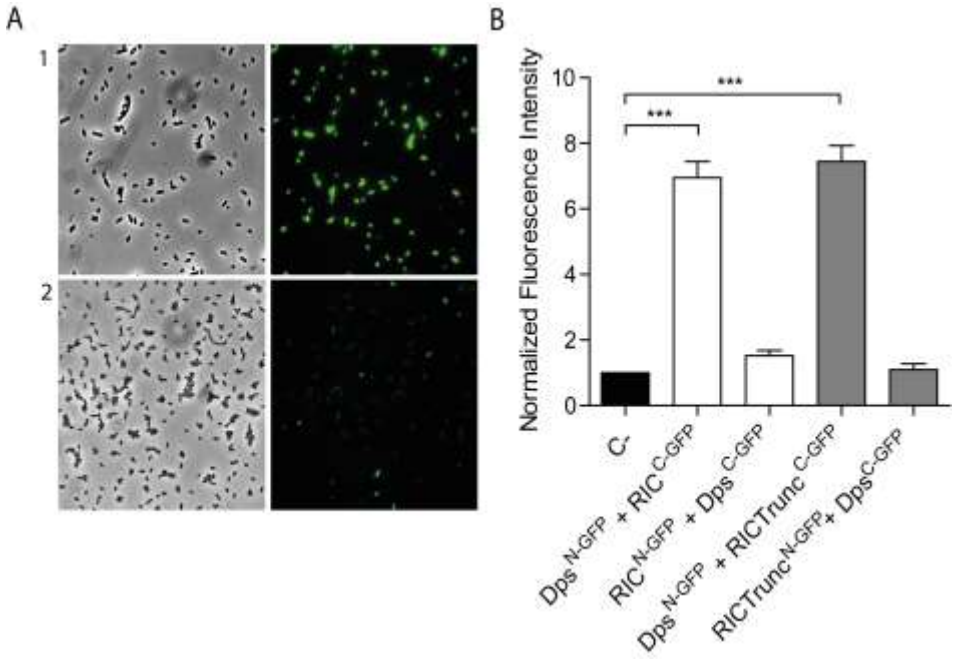


631

632 **Figure 3: Analysis of the interaction the *E. coli* RIC and Dps proteins by BiFC.** Cells
633 were co-transformed with vectors expressing either $RIC^{C\text{-}GFP}$ (pMRBAD-link-C-GFP-RIC)
634 or $RIC\text{-}Truncated^{C\text{-}GFP}$ (pMRBAD-link-C-GFP-RICTrunc) with $Dps^{N\text{-}GFP}$ (pET11a-link-N-
635 GFP-Dps). Dps-RIC protein interactions were assessed by BiFC assay. The inverse
636 configurations were also included. A) Cells expressing $RIC^{C\text{-}GFP}$ and $Dps^{N\text{-}GFP}$ analysed by
637 light microscopy (bright field, left upper panel) and fluorescence microscopy (right upper
638 panel). Lower panels depict images of cells co-transformed cells with empty vectors.
639 Images were acquired using a 100x objective and a FITC filter was used for the acquisition
640 of the fluorescence images. B) Fluorescence quantification was achieved using MetaMorph
641 Microscopy Automation and Image Analysis Software. Fluorescence values for negative
642 control (empty plasmid vectors) were normalized to 1. Values are means ± standard error of
643 at least three independent cultures analysed in duplicate ***$p<0.0005$ (One-way ANOVA
644 multiple comparison test).

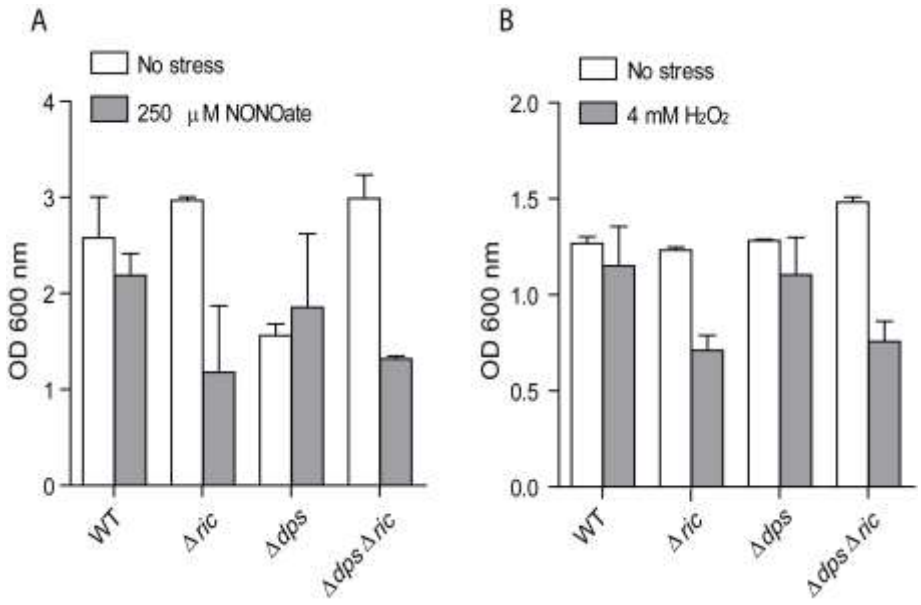


**Figure 4: Growth impairment caused by nitrosative and oxidative stress is related to *ric* absence.** *E. coli* wild type, Δ*ric*, Δ*dps* and Δ*dps*Δ*ric* strain were grown under anaerobic (A) and aerobic (B) conditions. At an $OD_{600}$=0.3, cells were left untreated (white bars), treated (grey bars) with 250 µM spermine NONOate for 7 h (A), or treated with 4 mM $H_2O_2$ for 5 h (B). Error bars are ± SD for experiments carried out at least three times.

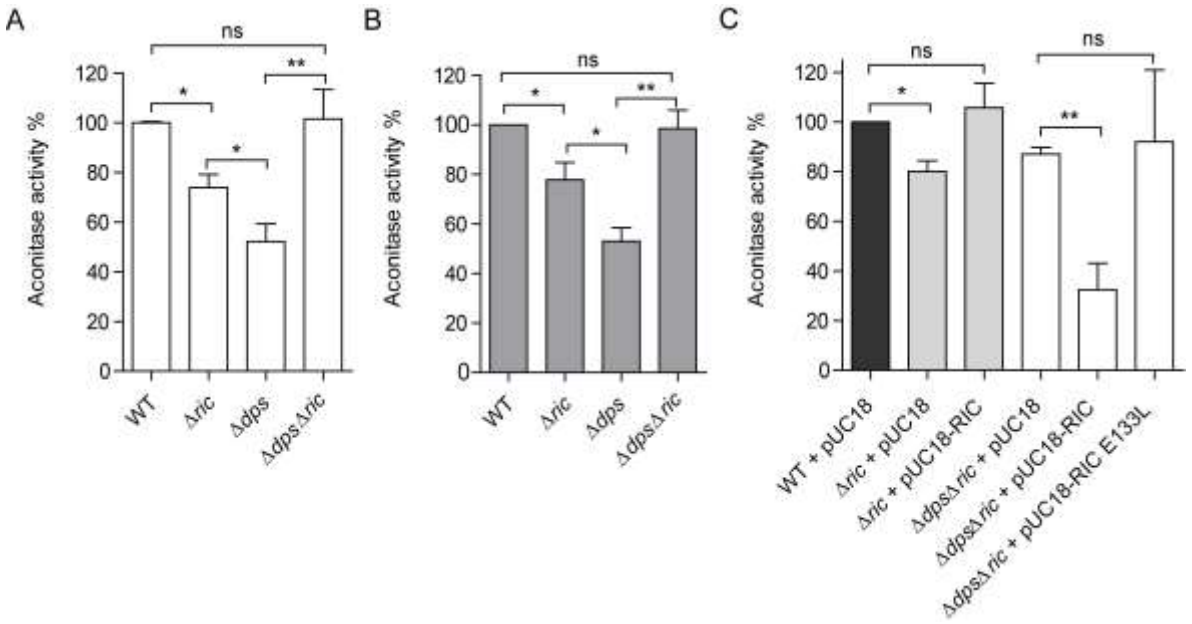


**Figure 5: Effect of Δ*dps* and Δ*ric* mutations on aconitase activity.** Aconitase activity of *E. coli* wild type, Δ*ric*, Δ*dps* and Δ*dps* Δ*ric* strains grown aerobically to $OD_{600}$ 0.6 (A, C) or 2.0 (B). Complementation experiments (C) were performed for the Δ*ric* and Δ*dps* Δ*ric* strains by transformation with pUC18 or with pUC18 encoding the RIC protein or Glu133Leu-RIC (a RIC protein where glutamate 133 was site-directed mutated by leucine (9)). Values are represented as normalized to the aconitase activity of wild type cells. Values are means (± standard error) of at least two independent cultures analysed in duplicate. *p<0.05; **p<0.005; ns: not significant (unpaired Student's t-test).

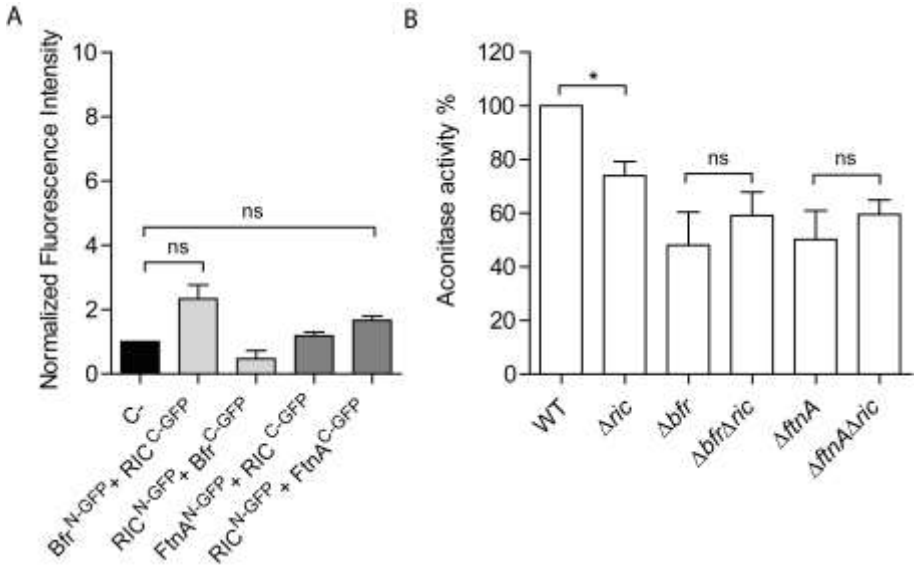


666

667 **Figure 6: Analysis of interaction between the iron-storage proteins, Bfr and FtnA, and**
668 **the RIC protein, and impact of iron-storage proteins on the RIC-protein dependence**
669 **of aconitase activity.** (A) Possible protein interaction between RIC and Bfr ant FtnA was
670 analysed by fluorescence microscopy and quantified by MetaMorph Microscopy
671 Automation and Image Analysis Software. Cells were co-transformed with vectors
672 expressing $RIC^{C\text{-}GFP}$ (pMRBAD-C-GFP-RIC) and $Bfr^{N\text{-}GFP}$ (pET11a- N-GFP-Bfr) or $FtnA^{N\text{-}GFP}$
673 (pET11a-N-GFP-FtnA). The inverse conformations were also tried. Fluorescence values
674 for negative control (empty plasmid vectors) were normalized to 1. Values are means ±
675 standard error of at least three independent cultures analysed in duplicate. ns: not
676 significant (One-way ANOVA multiple comparison test). (B) *E. coli* cells of single (Δ*ric*,
677 Δ*bfr*, Δ*ftnA*) and double mutant strains (Δ*bfr* Δ*ric*, Δ*ftnA* Δ*ric*) were grown aerobically,
678 collected at OD=0.6 and its aconitase activity determined. Values are represented as
679 normalized to the aconitase activity of wild type cells. Values are means ± standard error of
680 at least two independent cultures analysed in duplicate. *$p<0.05$; ns: not significant
681 (unpaired Student's t-test

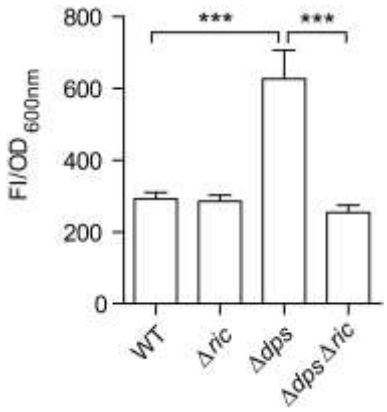


**Figure 7: Impact of Δ*dps* and Δ*ric* mutations on intracellular ROS levels.** The *E. coli* wild type and isogenic Δ*ric*, Δ*dps* and Δ*dps* Δ*ric* mutant strains were grown to OD 0.6 and the intracellular ROS levels were measured by incubation of cell suspensions with 10 µM DCFH-DA for 2 h. Fluorescence intensity was normalized according to the final OD (FI/OD). Values are means (± standard error) of at least three independent cultures analysed in duplicate. ***p<0.0005 (unpaired Student's t-test).

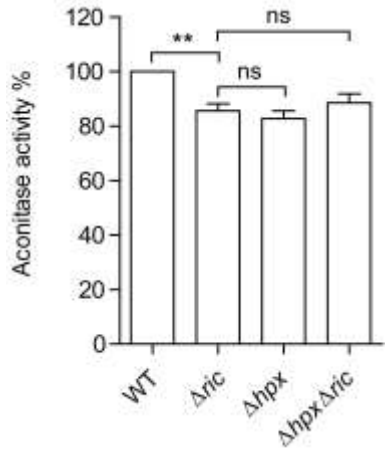


**Figure 8: Effect of combining the Δ*hpx* and Δ*ric* mutations on aconitase activity.** Aconitase activity of the *E. coli* wild type, Δ*ric*, Δ*hpx* (Δ*ahpCF* Δ*katE* Δ*katG*), and Δ*hpx* Δ*ric* strains cultured aerobically to log phase ($OD_{600}$=0.6). Values are represented as normalized to the aconitase activity of wild type cells. Values are means (± standard error) of at least two independent cultures analysed in duplicate. ***p<0.0005; ns: not significant (unpaired Student's t-test).